Organizing Spectral Image Database Using Self-Organizing Maps

Oili Kohonen and Timo Jääskeläinen
Department of Physics, University of Joensuu, Joensuu, FINLAND

Markku Hauta-Kasari, Jussi Parkkinen▲
Department of Computer Science, University of Joensuu, Joensuu, FINLAND

Kanae Miyazawa
Department of Information and Computer Sciences, Toyohashi University of Technology, Toyohashi, JAPAN

Techniques for searching images from a spectral image database and calculating the distances between spectral images using different distance measures are proposed and the importance of the normalization that is based on the human visual sensitivity function is examined. The searching techniques are based on the use of one-and two-dimensional Self-Organizing Map (SOM). In the case of one-dimensional SOM, the Best Matching Unit (BMU) histogram is created for every spectral image of a database, and images are ordered according to the histogram dissimilarity. Two-dimensional SOM is trained by using spectral data and BMU-histograms as a training data and the distance between spectral images is defined based on the histogram dissimilarity and image locations on the map, respectively. The proposed techniques are useful in image search and the order of the database is different for spectral images and for spectral images weighted by human visual sensitivity function. The order of the database is also highly dependent on the used distance measure. The results using a real spectral image database are given.

Journal of Imaging Science and Technology 49: 431–441 (2005)

Introduction

Spectral imaging has faced growing interest during the last few years. Especially the development of computer-based multimedia systems has created a real need to reproduce color precisely under different illuminations. Even though metameric imaging is a cheap and practical way to achieve a color match for a certain illumination, spectral imaging is needed to achieve a color match for all observers across the changes in illumination.

High data volume is a significant disadvantage of spectral imaging. In metameric imaging only three channels are needed, but in spectral imaging the number of channels used varies from four to several hundreds, depending on needed spectral resolution. When the spectral range is from 400 nm to 700 nm, typical numbers of channels are 31 and 61.

Image retrieval from conventional image databases has been actively under research since the early 1990's.[1] Many efficient techniques such as PicSOM,[2,3] QBIC,[4] CANDID,[5,6] CBIR,[7,8] NETRA,[9] Photobook,[10] COMPASS[11] and MARS[12] have been developed for RGB image databases. At the moment only a few spectral image databases are publicly available, but the number and size of them are expected to increase in the future due to the rapid development of spectral imaging systems.[13] For example Munsell Color Science Laboratory provides a spectral image database that is called Lipp-mann2000[14], and also the University of Joensuu[15] has started to put out some spectral images for research purposes. In consequence of the high data volume of spectral images, fast methods for searching images in the spectral image databases will be needed.

A searching technique in a spectral image database using one-dimensional Self-Organizing Map (SOM) was originally proposed by Hauta-Kasari et al. in Ref. 13. There a Best-Matching Unit (BMU) histogram was defined, and a query from a database was realized according to the BMU-histogram dissimilarity that was calculated using Euclidean distance as a distance measure. In our previous study[16] the size of the database and the number of similarity measures were increased. In addition, the idea of the human visual sensitivity function based normalization and the use of a BMU-histogram-trained two-dimensional self-organizing map (SOM) were proposed. The use of the human visual sensitivity function arose from the fact that the results of database searches are evaluated by human beings watching

Original manuscript received July 13, 2004

▲ IS&T Member

Supplemental Material— Figures 4 and 6–14 can be found in color on the IS&T website (www.imaging.org) for a period of no less than two years from the date of publication.

Corresponding Author: O. Kohonen, Oili.kohonen@joensuu.fi

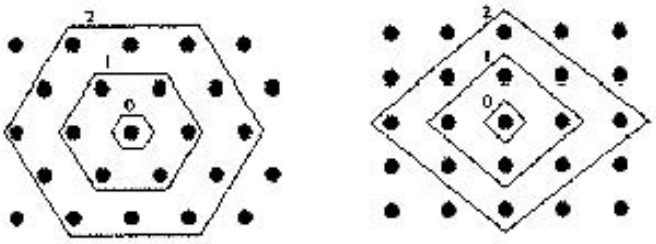

Figure 1. Neighborhoods of the centermost unit: hexagonal lattice on the left, rectangular on the right.[26]

the ordered outputs. In this study the importance of the proposed normalization is examined more carefully, and two new similarity measures are introduced.

Principles of SOM

In this study the spectral images are represented by histograms which are used as feature vectors in the proposed spectral database organizing method. For histogram generation, the order of the pixel values must be known. For grayscale images, there exists a certain intensity-based order for the gray levels, i.e., for pixels with scalar value. The situation is different when we deal with spectral images, where the pixel values are color spectra, i.e., vectors. There is no natural ordering for the color spectra. However, the use of self-organizing maps enables us to gain an order for multi-dimensional data. In Ref. 17 SOMs have already been successfully used for ordering color spectra. In this study the same method as in Ref. 17 was used for histogram generation.

The Self-Organizing Map[18] algorithm is an unsupervised learning algorithm that defines a mapping from a high-dimensional input data space into a lower-dimensional space. Inputs that are located close to each other in a high-dimensional space are also located near to each other in a new, lower-dimensional space. SOM consists of arranged units (or neurons) which are represented by weight vectors. It is worth noticing that the dimension of input data vectors and the dimension of weight vectors are the same. The units of the map are connected to adjacent units by a neighborhood relation, which dictates the topology of the map. The hexagonal and rectangular lattice structures with 0–, 1– and 2–neighborhoods are shown in Fig. 1.

At each training step one input data vector, x, is chosen from the training data set. The best matching unit (BMU) is defined as follows:

$$\|x - w_{\mathrm{BMU}}\| = \min_i \|x - w_i\|, \tag{1}$$

in which w_i and w_{BMU} indicate the weight vector of ith unit and the best matching unit, respectively. In a training phase, Euclidean distance is a distance measure typically used. The unit which produces the smallest distance is called a best matching unit for an input data vector x. After finding the BMU, the weight vectors are updated using the following equation:

$$w_i(t+1) = \begin{cases} w_i(t) + \alpha(t)\left[x(t) - w_i(t)\right], & \text{if } i \in N_{BMU}(t) \\ w_i(t), & \text{otherwise} \end{cases} \tag{2}$$

in which t denotes time. $N_{\mathrm{BMU}}(t)$ is a decreasing neighborhood function around the BMU and $\alpha(t)$ is a decreasing learning rate, for which $0 < \alpha(t) < 1$ holds.[19,20] The iterative training of SOM is described below in an algorithmic form.

Algorithm 1

Begin
    Initialize the SOM
    for i = 1 to number of epochs
        take input vector xrandomly from the training data
        find the BMU, w_{BMU}, for x by using the Eq. (1)
        update the weight vectors, w_i, of the map by using the Eq. (2)
        decrease the learning rate $\alpha(t)$ and neighborhood function $N(t)$
    end
End

The SOM can be considered as a $b \times c \times a$ matrix, in which b and c correspond to the spatial dimensions and a is a dimension of input data. In the case of a one-dimensional SOM $b = 1$ and $c > 1$ or vice versa. When $b > 1$ and $c > 1$ one deals with a two-dimensional SOM.

Searching Technique

For searching, the training data for SOM is created by selecting spectra from the chosen spectral images. Spectra are selected randomly and the number of spectra is chosen empirically. The training is performed as described in Algorithm 1.

After training, a BMU-histogram for a spectral image is created by the following way. The BMU is calculated for each pixel of a spectral image. As a result, we get a BMU-image, where each pixel is represented by an index number that corresponds to w_{BMU}. A histogram of the BMU-image is generated and normalized by the number of pixels in the image. The histogram generated represents the numbers distribution of different index numbers. That is to say, the distribution of the BMUs found. This process is done for each spectral image of a database, and a database of BMU-histograms is obtained as a result. The size of the histogram database matrix is $n \times m$, in which n and m are the number of spectral images used and the number of map units, respectively.

The search in a spectral image database using a one-dimensional SOM is done as follows. A spectral image is selected and its BMU-histogram is generated using the map by which the existing BMU-histogram database was generated. Next, the created BMU-histogram is compared with the histogram database. The distances between the histograms are calculated and the images are ordered according to these distances. If the selected image is included in the database, the smallest distance is 0. The results of the search are shown to a user as RGB-images. A diagram for ordering the spectral images using a one-dimensional SOM is shown in Fig. 2.

In the case of a two-dimensional SOM, there are two different ways to produce a SOM-map. In the first case, the spectral data is used as a training data, and the two-dimensional SOM is constructed by the same way as the one-dimensional SOM. In the other case the one-dimensional SOM is trained first, as described above, and the BMU-histogram database is generated. Next, these BMU-histograms are used as training data for the two-dimensional SOM. The search in this histogram-trained, two-dimensional SOM is done as follows. The spectral image is selected and its BMU-histogram is generated by using the one-dimensional SOM. Next, the

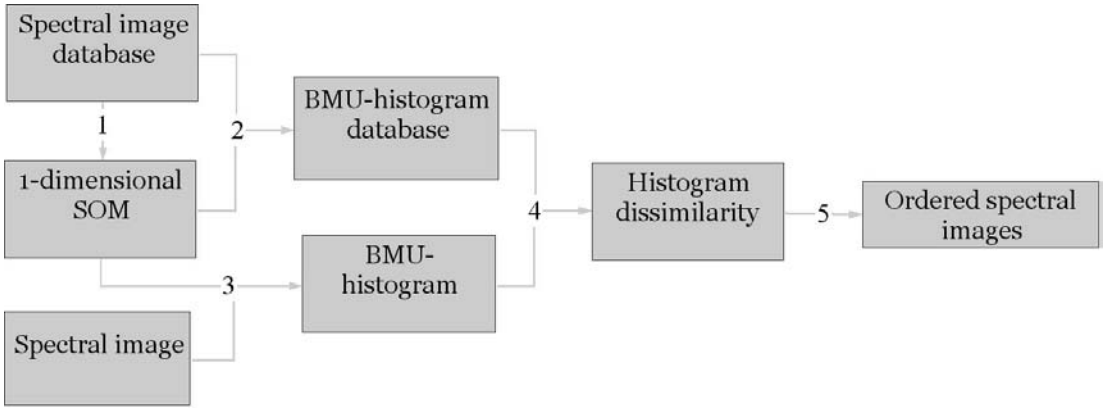

Figure 2. A diagram for ordering the spectral images using a one-dimensional SOM.

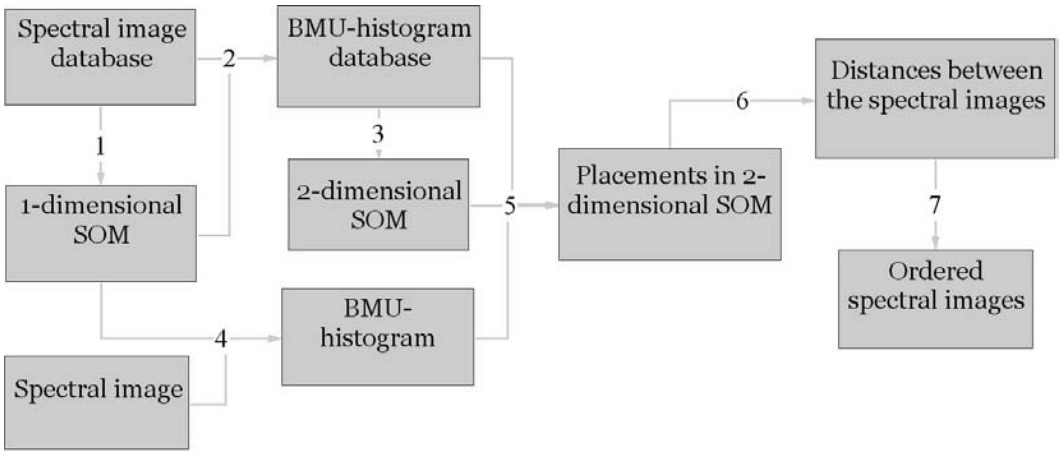

Figure 3. A diagram for ordering the spectral images using a BMU-histogram-trained two-dimensional SOM.

positions of this BMU-histogram and every histogram of a BMU-histogram database are located in the two-dimensional SOM. This is done by calculating the BMUs for the BMU-histograms. From now on these new BMUs are called the second level BMUs. In the case of the two-dimensional, histogram-trained SOM, the distances between the selected image and the images presented in a BMU-histogram database are calculated as a difference between the weight vectors that correspond to the calculated second level BMUs. A diagram for ordering the spectral images by using a histogram-trained, two-dimensional SOM is shown in Fig. 3. If the selected image is included in the database, or if any other image in the database has the same second level BMU as the selected image, the smallest distance is zero.

Distance Calculations

Distance calculations are done using Euclidean distance, energy, maximum peak location, Kullback–Leibler distance, dynamic partial distance and Jeffrey divergence as distance measures. The distances between two histograms, H_1 and H_2, in these metrics are described as follows:

$$\text{EuclideanDistance} = \sqrt{\sum_{i=1}^{m} \left(H_1(i) - H_2(i)\right)^2}, \quad (3)$$

$$\text{Energy} = \left| \sum_{i=1}^{m} H_1(i)^2 - \sum_{i=1}^{m} H_2(i)^2 \right|, \quad (4)$$

$$\text{MaximumPeakLocation} = \left| L_1 - L_2 \right|. \quad (5)$$

in which L_1 and L_2 are the indices of the maximum values of compared histograms.

$$\text{Kullback} - \text{LeiblerDistance} = \sum_{i=1}^{m} H_1(i) \log \frac{H_1(i)}{H_2(i)}, \quad (6)$$

$$\text{DynamicPartialDistance} = \left(\sum_{i \in k} \left| H_1(i) - H_2(i) \right|^{\lambda} \right)^{\frac{1}{\lambda}}, \quad (7)$$

Figure 4. Ordered output for spectral images in the case of one-dimensional SOM. The distance measure used is Euclidean distance. *Supplemental Material— Figure 4 can be found in color on the IS&T website (www.imaging.org) for a period of no less than two years from the date of publication.*

where k is a set that contains $\leq m$ components of the feature space with the smallest values for $|H_1(i) - H_2(i)|$, $k = 1, \ldots, m$; λ can be chosen, and m is a dimension of the histograms. If $k = m$, Manhattan distance and Euclidean distance are obtained by setting $\lambda = 1$ and $\lambda = 2$, respectively.

$$\text{JeffreyDivergence} = \sum_{i=1}^{m}\left(H_1(i)\log\frac{H_1(i)}{H_3(i)} + H_2(i)\log\frac{H_2(i)}{H_3(i)}\right). \quad (8)$$

where $H_3 = H_1 + H_2/2$ is the mean histogram.[21–23]

Spectral Image Database

In this study a database of 106 spectral images was used. The images have been measured at the University of Joensuu (Finland),[15] Lappeenranta University of Technology (Finland), Chiba University (Japan), Saitama University (Japan), University of Bristol (United Kingdom) and at the Marine Biological Laboratory (Maryland, USA). The images have been filtered into equal format: 61 spectral components with the spectral range from 400 nm to 700 nm at 5 nm intervals. The size of the images varies from 3 megabytes to 56 megabytes.

TABLE I. The Objects of the Spectral Image Database

Objects	Number	Types of images	Number of images
skin	11	printed magazine pictures	8
corals	10	logos of business cards	3
plants	40	synthetic images	24
scenery	8	other	2

The objects of the database are listed in Table I. In addition to measured spectral images, there are 24 synthetically created images of which half have the same texture but different color and the other half have the same green color but different texture. The synthetic images have been generated using the virtual texture coloring technique described in Ref. 24. These images were generated for future work, in which the texture features will be studied. At the moment we do not have this kind of data as natural spectral images. The images of the database can be seen in grayscale in Fig. 4 (color version of Fig. 4 can be found as Supplemental Material), which shows the ordered output for spectral images in the case where Euclidean distance is used as a distance measure.

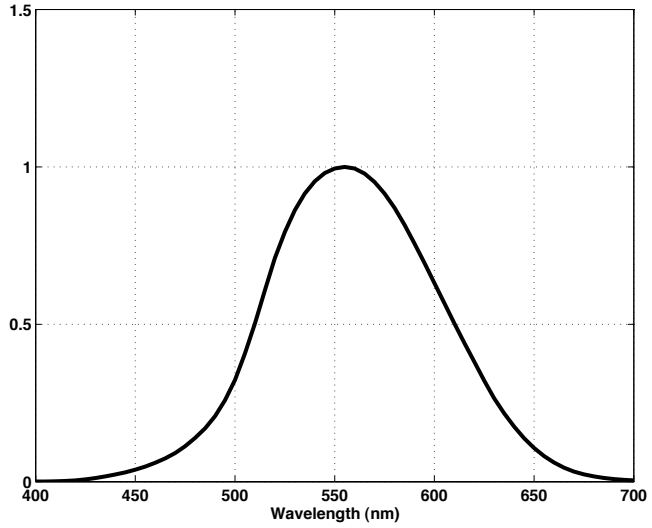

Figure 5. The human visual sensitivity function.[27]

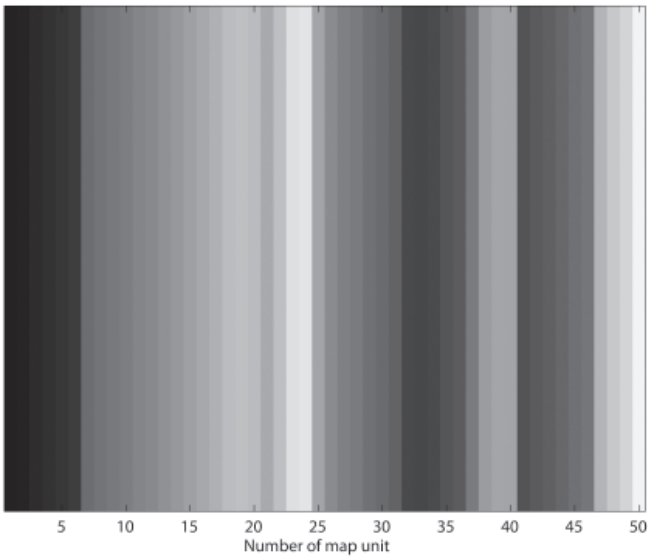

Figure 6. Weight vectors of one-dimensional SOM converted to RGB colors. Vertical lines correspond to the map units. *Supplemental Material— Figure 6 can be found in color on the IS&T website (www.imaging.org) for a period of no less than two years from the date of publication.*

Experiments

The calculations were done using a SOM PAK-software package[19] and a SOM toolbox for Matlab.[25,26] SOM-maps were created by using spectral images and images weighted by the human visual sensitivity function[27] (shown in Fig. 5) to study the importance of the normalization earlier proposed. In all cases the topology type used in the map was hexagonal and the learning rate function type was linear. When a one-dimensional SOM is in question the hexagonal topology corresponds to the rectangular topology. The dimensions of the weight vectors in the cases, where spectral data and BMU-histogram data were used as a training data, were 61 and 50, respectively. In the cases of one-and two-dimensional spectral data-trained SOMs, 10,000 spectra from each image were selected randomly as a training data. To retain a theoretical possibility that every spectrum included in the training data could be chosen at least once, the minimum number of epochs has to be more than 1,000,000.

The one-dimensional SOMs, consisting of 50 units, were trained by using 2,000,000 epochs in the ordering phase and 4,000,000 epochs in the fine tuning phase. The unit size of the SOM was chosen empirically as in Ref. 17. The initial radius of the training area was 50 and the learning rates in the ordering phase and in the fine tuning phase were 0.9 and 0.02, respectively. The histogram similarities were calculated by using Euclidean distance, energy, maximum peak location, Kullback–Leibler distance, dynamic partial distance and Jeffrey divergence as distance measures, and the spectral images were ordered according to the dissimilarities. In the equation of dynamic partial distance, the 25 smallest distances ($k = 25$) between the compared histograms were taken into account, and $\lambda = 2$.

The weight vectors that correspond to the units of the one-dimensional SOM are shown in RGB colors in the Fig. 5. The ordered outputs for images in the case of Euclidean distance are shown in Figs. 4 and 7. The portrait image of a young lady, shown in the left upper corner, is used as a reference image and the images from left to right and from top to down are the images in an ascending order according to dissimilarity. It can be seen that ordering using spectral images differs from the one in which the images weighted by human visual sensitivity function are used. The results in the cases of other similarity measures are shown in Figs. 8 and 9. (Due to the restricted amount of a space, only the first 10 images of the search results are shown.) In the cases where Euclidean distance and dynamic partial distance are used, the better results are gained by using normalization, but in the case of Jeffrey divergence, the opposite holds true. When Kullback–Leibler distance, energy, or maximum peak location are used as distance measures, the results for weighted images are slightly better. According to these results it cannot be said that the use of the human visual sensitivity function would generally lead to better results.

Next, the two-dimensional SOMs were trained using spectral data as training data. Again, both the spectral images and the images weighted by the human visual sensitivity function were used. All parameters except the number of neurons were the same as in the case of one-dimensional SOMs. The number of neurons was lowered by one and the sizes of the maps produced were 7×7 neurons. The ordered outputs for images in the cases of non-weighted and weighted images using Euclidean distance, energy, Kullback–Leibler distance, maximum peak location, dynamic partial distance and Jeffrey divergence are shown in Figs. 10 and 11, respectively. It can be seen that ordering using spectral images differs from that, in which images weighted by the human visual sensitivity function are used. Generally it seems that better results are achieved by using the non-weighted images. However, it is worth noticing that the results are evaluated by human beings. By comparing these results to the results from one-dimensional SOM feature by feature, it can be seen that the spectral data-trained, two-dimensional SOM gives better results in the case of non-weighted images, when Euclidean distance and dynamic partial distance are used. In the case of Jeffrey divergence the situation is opposite. Energy, Kullback–Leibler distance and maximum peak location give quite bad re-

Figure 7. Ordered output for spectral images weighted by human visual sensitivity function in the case of one-dimensional SOM. The distance measure used is Euclidean distance. *Supplemental Material— Figure 7 can be found in color on the IS&T website (www.imaging.org) for a period of no less than two years from the date of publication.*

sults despite of the dimensionality of the map and the normalization. When the weighted images are used, the use of the one-dimensional SOM seems to be more reasonable.

Finally, a two-dimensional SOM was constructed using a BMU-histogram database for weighted images as a training data. The histogram database used was created on the basis of the one-dimensional SOM. The size of the resulting map was (20 $\times$ 20) units. The unit number is that high because we did not want many images to have the same second level BMU. The initial radius of the training area was 20 and the learning rates in the ordering phase and in the fine tuning phase were 0.9 and 0.02, respectively. The second level BMUs for the BMU-histogram database were calculated using Euclidean distance as a distance measure. The images were placed into the two-dimensional map according to the second level BMUs. The distances between the chosen reference image and every image in the database were calculated as a difference between weight vectors that correspond to the calculated second level BMUs in the BMU-histogram-trained, two-dimensional SOM.

Due to the restricted amount of space, the whole two-dimensional SOM that contains the images cannot be shown. A small part of it is shown in Fig. 12. The ordered outputs, based on the distance calculations inside the map, are shown in Fig. 13. The best results are obtained using the maximum peak location. The resulting "balcony" and "cream cake" images can be explained by the fact that the reference image as well as these images were originally measured from printed magazines for which the paper type used is quite similar.

An example of the connections between the spectral images and BMU-histograms is shown in Fig. 14. The figure contains histograms for 5 non-weighted and weighted spectral images. The shapes of the histograms are spikier and the locations of the peaks are more similar between each other in the case of the weighted images. Also the structure of the histograms seems more periodic for the weighted images. These are consequence of the fact that multiplication by the human visual sensitivity function weights some certain spectral channels of the images very strongly.

Discussion

A searching technique in a spectral image database with six different distance measures for the cases of one-and two-dimensional SOMs was implemented and the importance of the human visual sensitivity function normalization was tested. In addition, a technique for cal-

Figure 8. Ordered output for spectral images in the case of one-dimensional SOM. The distance measures used, row by row from top to down are: energy, Kullback–Leibler distance, maximum peak location, dynamic partial distance and Jeffrey divergence. *Supplemental Material— Figure 8 can be found in color on the IS&T website (www.imaging.org) for a period of no less than two years from the date of publication.*

Figure 9. Ordered output for spectral images weighted by human visual sensitivity function in the case of one-dimensional SOM. The distance measures used, row by row from top to down are: energy, Kullback–Leibler distance, maximum peak location, dynamic partial distance and Jeffrey divergence. *Supplemental Material— Figure 9 can be found in color on the IS&T website (www.imaging.org) for a period of no less than two years from the date of publication.*

Figure 10. Ordered output for spectral images in the case of two-dimensional, spectral data-trained SOM. The distance measures used, row by row from top to down are: Euclidean distance, energy, Kullback–Leibler distance, maximum peak location, dynamic partial distance and Jeffrey divergence. *Supplemental Material— Figure 10 can be found in color on the IS&T website (www.imaging.org) for a period of no less than two years from the date of publication.*

Figure 11. Ordered output for weighted spectral images in the case of two-dimensional, spectral data-trained SOM. The distance measures used, row by row from top to down are: Euclidean distance, energy, Kullback–Leibler distance, maximum peak location, dynamic partial distance and Jeffrey divergence. *Supplemental Material— Figure 11 can be found in color on the IS&T website (www.imaging.org) for a period of no less than two years from the date of publication.*

Figure 12. The locations of spectral images in two-dimensional, BMU-histogram-trained SOM.. *Supplemental Material—Figure 12 can be found in color on the IS&T website (www.imaging.org) for a period of no less than two years from the date of publication.*

culating the distances between spectral images using a BMU-histogram-trained, two-dimensional SOM was proposed, and spectral images were ordered by these distances.

It was shown that the proposed features are useful in image search. The order of the database is different for spectral images and for spectral images weighted by the human visual sensitivity function. Also, the order of the database is highly dependent on the distance measure used. According to these results, it is impossible to say whether or not normalization using the human visual sensitivity function should be used. Furthermore these results are strictly valid only for the database used.

Euclidean distance, energy, maximum peak location, Kullback–Leibler distance, dynamic partial distance and Jeffrey divergence were used as distance measures. Each of these metrics has advantages and disadvantages, and it cannot be said that one certain measure should be transcendent compared to the others. All distance measures used, except energy, are based on bin-by-bin comparisons. The problem with bin-by-bin comparisons is that the histograms of similar images are not always similar with respect to every histogram component. Bin-by-bin-based distance measures are highly position dependent and even a very small shift in a histogram may cause a larger distance estimate even though the shapes of the compared histograms may be very similar. On the other hand, the distance estimate between two histograms that may have very different shapes may be quite small for the case of energy, which is the only distance measure that is not based on bin-by-bin comparisons. In the case of energy the only thing that matters, is the distribution of the values in the histogram; i. e., the heights of the peaks are important but the locations of the peaks are totally irrelevant.

Drawbacks of the proposed techniques are that the training phase of SOM takes quite a long time, and the size of the training data is large. In conclusion, the main results of this article are proposed searching techniques. After the training phase of SOM, the techniques are fast and memory efficient enough to be used for searching spectral images in a database.

The next goal of this research is to include the textural features to the proposed methods, study the influence of the image background, and combine some distance measures. Also the use of the topological neighborhood of the SOM units in histogram comparisons is to be included. At the moment, the Euclidean distance is used as a distance measure in the training phase. It is hard to say whether this is unfair to the other dis-

Figure 13. Ordered output for spectral images weighted by human visual sen-sitivity function in the case of two-dimensional, BMU-histogram-trained SOM. The used distance measures row by row from top to down are: Euclidean distance, energy, Kullback–Leibler distance, maximum peak location, dynamic partial distance and Jeffrey divergence. *Supplemental Material— Figure 13 can be found in color on the IS&T website (www.imaging.org) for a period of no less than two years from the date of publication.*

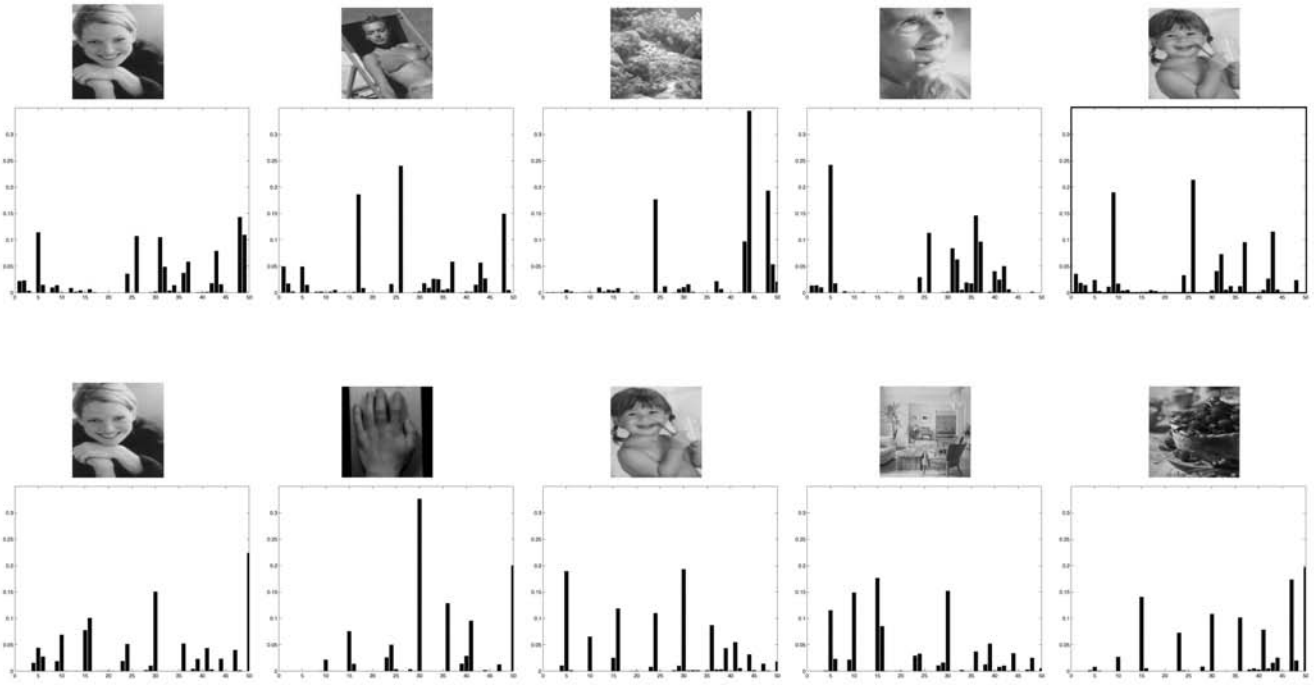

Figure 14. Example of the BMU-histograms that represent spectral images. Upper and lower histogram rows represents spectral images and spectral images weighted by human visual sensitivity function, respectively. *Supplemental Material— Figure 14 can be found in color on the IS&T website (www.imaging.org) for a period of no less than two years from the date of publication.*

tance measures. However, in the future, other measures will be used in the training phase as well.

References

1. S. Brandt, J. Laaksonen and E. Oja, "Statistical Shape Features in Content-Based Image Retrieval", *Proc. 15th International Conference on Pattern Recognition*, (ICPR, Barcelona, Spain, 2000), p. 1066.
2. J. Laaksonen, M. Koskela, S. Laakso, and E. Oja, "Self-Organizing Maps as a Relevance Feedback Technique in Content-Based Image Retrieval", *Pattern Anal. Appl.* ISSN: 1433-7541, **4,** 140 (2001).
3. M. Koskela, J. Laaksonen, S. Laakso, and E. Oja, *The PicSOM Retrieval System: Description and Evaluations, The Challenge of Image Retrieval,* (University of Brighton,Brighton, UK, 2000).
4. QBIC–IBM's Query By Image Content: http://wwwqbic.almaden.ibm.com/(June 26, 2004).
5. The CANDID Project 1994–1996: http://public.lanl.gov/kelly/CANDID/index.shtml (June 29, 2004).
6. P. M. Kelly, M. Cannon and J. E. Barros, "Efficiency issues related to probability density function comparison", *Proc. SPIE* **2670,** 42 (1996).
7. http://www.ep.liu.se/databases/cse-imgdb/ (June 29, 2004).
8. L. V. Tran, *Efficient Image Retrieval with Statistical Color Descriptors*, Linköping Studies in Science and Technology Dissertation No. 810, (Department of Science and Technology, Linköping University, Norrköping, Sweden, May 2003); http://www.ep.liu.se/diss/science technology/08/10/digest.pdf (June 29, 2004).
9. http://maya.ece.ucsb.edu/Netra/ (June 29, 2004).
10. http://vismod.www.media.mit.edu/vismod/demos/photobook/index.html (June 28, 2004).
11. http://compass.itc.it/ (June 29, 2004).
12. http://www-db.ics.uci.edu/pages/research/mars.shtml (June 26, 2004).
13. M. Hauta-Kasari, K. Miyazawa, J. Parkkinen, and T. Jääskeläinen, "Searching Technique in a Spectral Image Database", *13th Scandinavian Conference on Image Analysis*, J. Bigun and T. Gustavsson, Eds., in *Lecture Notes in Computer Science* **2749,** 927 (2003).
14. Lippmann2000: A spectral image database under construction http://www.cis.rit.edu/mcsl/online/lippmann2000.shtml (June 27, 2004); http://www.cis.rit.edu/mcsl/online/Spectral/TechnicalPapers/Lippmann2000 Chiba Oct1999.pdf (June 27, 2004).
15. http://spectral.joensuu.fi/ (June 27, 2004)
16. O. Kohonen, M. Hauta-Kasari, K. Miyazawa, J. Parkkinen, and T. Jääskeläinen, "Methods to organize spectral image database", *Proc. 2nd CGIV Conference*, (IS&T, Springfield, Va, 2004), p. 372.
17. K. Miyazawa, J. Hakkarainen, J. Parkkinen, and T. Jääskeläinen, "Ordering of color spectra for digital image enhancement", in *Proc. ICPS '02*, (SPSTJ, Tokyo, Japan, 2002), p. 492.
18. T. Kohonen, *Self-Organizing Maps*, 3rd ed., Springer Series in Information Sciences, Vol. 30, Springer, Berlin, 2001.
19. T. Kohonen, J. Hynninen, J. Kangas, and J. Laaksonen, "SOM PAK: The Self-Organizing Map Program Package", Technical Report A31, Helsinki University of Technology, Laboratory of Computer and Information Science, (1996).
20. E. Alhoniemi, J. Hollmen, O. Simula, and J. Vesanto, "Process Monitoring and Modelling Using the Self-Organizing Map" in *Integrated Computer-Aided Engineering*, ISSN: 1068-2509, **6,** 3–14 (1999).
21. T. Ojala, M. Pietikäinen and D. Harwood, "A comparative study of texture measures with classification based feature distributions", *Pattern Recognition*, ISSN: 0031-3203, **29,** 51 (1996).
22. B. Li, E. Chang and C.-T. Wu, "DPF–A perceptual distance function for image retrieval", *Proc. ICPS '02*, (SPSTJ, Tokyo, Japan, 2002), p. 597.
23. J. Puzicha, Y. Rubner, C. Tomasi, and J. Buhmann, "Empirical evaluation of dissimilarity measures for color and texture", *Proc. IEEE, Int'l. Conf. on Computer Vision*, (IEEE Press, Los Alamitos, 1999), p. 1165.
24. V. Botchko, S. Nakauchi, J. Parkkinen, and H. Kälviäinen, "Multispectral texture derivation in virtual coloring", in *Texture Analysis in Machine Vision*, M. Pietikäinen, Ed., (World Scientific Publishing Co., Singapore, 2000).
25. SOM Toolbox, a software package for Matlab 5: http://www.cis.hut.fi/projects/somtoolbox/ (June 28, 2004)
26. J. Vesanto, J. Himberg, E. Alhoniemi, and J. Parhankangas, "Self-organizing map in Matlab: the SOM toolbox", *Proc. Matlab DSP Conference*, (Comsol Oy, Espoo, Finland, 1999), p. 35.
27. G. Wyszecki and W. S. Stiles, *Color Science*, (Wiley, New York, 1982).